Novel Branching Topology in Polyethylenes As Revealed by Light Scattering and ^{13}C NMR

Patricia M. Cotts,* Zhibin Guan, Elizabeth McCord, and Steve McLain

DuPont Central Research, Experimental Station, Wilmington, Delaware 19880

Received May 26, 2000; Revised Manuscript Received July 11, 2000

ABSTRACT: A group of polyethylenes synthesized using palladium α-diimine catalysts were studied using ^{13}C NMR spectroscopy, intensity light scattering, dynamic light scattering, and viscometry. These catalysts are known to produce branched polyethylenes without α-olefin comonomers. The series of polymers studied were synthesized under conditions of varying ethylene pressure. The polymers are highly branched and completely amorphous and are thus soluble in common organic solvents at ambient temperatures. Light scattering determinations of the root-mean-square radius of gyration (R_g) and the molecular weight M of fractions eluting from a size exclusion chromatograph demonstrated that, at a given M, R_g decreased as ethylene pressure decreased. The hydrodynamic parameters—the Stokes radius (R_H) from dynamic light scattering and the intrinsic viscosity ([η])—also decreased. The change in R_g at a constant M results from the change in branching topology for the polymers synthesized at different ethylene pressures. The parameter R_g^2/M varies by an order of magnitude for the polymers synthesized under ethylene pressures varying from 0.1 atm to 500 psi. However, the total branching (methyls per 1000 CH_2) and the distribution of short branches (methyl, ethyl, propyl, etc.) determined by ^{13}C NMR remained essentially unchanged. These observations indicate the branching topology changes with polymerization pressure. Polymer topology varies from predominantly linear with many short branches at higher ethylene pressures to a densely branched, arborescent globular structure at very low ethylene pressures. Polymers synthesized at the lowest ethylene pressure studied, 0.1 atm, exhibited dilute solution parameters similar to those observed for dendrimers or many-armed stars, with R_g/R_H below unity, and a segment density approaching that of a hard sphere.

Introduction

Commercial polyolefins synthesized by free radical polyerization typically can possess two types of branching: short chain branches (octyl and shorter, arising from intramolecular chain transfer and/or introduction of α-olefins) and long chain branches (arising from intermolecular chain transfer or incorporation of an olefin-terminated polymer chain) in which the branch is of length comparable to the backbone (greater than 100 carbons).[1] While the primary function of the short chain branches is reduction of crystallinity, the long chain branches can have a dramatic effect on rheological properties.[2] Branches of more regular length and distribution can be obtained with the more recent metallocene catalysts.[3]

Polymerization of ethylene using catalysts derived from late transition metals such as nickel(II) and palladium(II) has recently been reported by Brookhart and co-workers.[4] These catalysts incorporate very bulky chelating diimine ligands and have been shown to lead to substantially branched polymers without the use of comonomers via a chain walking mechanism involving a β-hydride elimination and a readdition process.[4−12] For Ni-catalyzed polymers, the degree of branching decreases with increasing ethylene pressure during synthesis.[10,11] For the Pd-catalyzed polymers, the degree of branching in terms of methyls per 1000 CH_2 appears essentially independent of ethylene pressure.[7−12] However, our previous studies have shown that the polyethylenes made with the Pd catalysts possess unique branch-on-branch topologies, which can be controlled by ethylene pressure during synthesis.[7,8] Synthesis with the Pd catalysts at high ethylene pressures produces a polymer of predominantly linear topology with many short branches: an amorphous, tough, elastomer in bulk. Synthesis at greatly reduced ethylene pressures produces a compact, densely branched polymer with substantially increased branch-on-branch structures: a viscous oil even at high molecular weight. In this study, we report detailed characterization of a group of seven polyethylenes synthesized using a palladium catalyst at ethylene pressures varying from above 500 psi to below 1 atm. All the polymers were highly branched, amorphous, and soluble in common organic solvents at ambient conditions. At higher ethylene pressures, solution properties were consistent with other soluble polyolefins containing large amounts of short chain branches, e.g., atactic polypropylene, poly(1-octene), etc.[13−16] At very low ethylene pressures, very compact structures were obtained, with solution properties approaching those of large dendritic structures, multiarmed stars, or hyperbranched polymers. The terminology *hyperbranched* arose from the synthesis of branched polymers using AB_2 monomers in which no gelation point is approached. While no gelation point is expected for the polymers reported here, the branching structure is different than that expected for AB_2 monomers. In contrast to a recently reported synthesis of hyperbranched polyethylene,[17] these polymers are of high molecular weight, with weight-average molecular weights M_w of 200 000−500 000.

Experimental Section

Polymer Synthesis. Polymerizations were carried out as described previously,[7,8] using (ArN=C(Me)−C(Me)=NAr)Pd-$(CH_2)_3$C(O)OMe]Barf (Ar = 2,6-$Me_2C_6H_3$) as the catalyst.[8] A typical polymerization was done as the following: A solution of 50 mg (33.9 μmol) of the Pd α-diimine catalyst in 100 mL of chlorobenzene was transferred into a 600 mL Parr pressure reactor under nitrogen. The reactor was heated to 35 °C, and the solution was stirred by a mechanical stirrer set at 500 rpm.

10.1021/ma000926r CCC: $19.00
Published on Web 08/25/2000

Ethylene was charged to the reactor to 1 atm. Polymerization was continued at 35 °C and 1 atm for 18.7 h. After terminating the polymerization, the solution was diluted with toluene, then passed through a column packed with alumina, silica gel, and Celite to remove the catalyst, and finally precipitated into a large excess of methanol. The polymer was collected and dried in vacuo to give PE as viscous oil or transparent, tough, elastomer.

Ethylene pressure was usually controlled by a gas regulator except for the 0.1 atm experiment. For the polymerization at 0.1 atm of ethylene, a mixture of ethylene and nitrogen (with a ratio of 1:9) was prepared and mixed well in a gas cylinder. The mixture was bubbled through a chlorobenzene solution of the Pd α-diimine catalyst at 1 atm total pressure. The partial pressure for ethylene was, therefore, 0.1 atm.

^{13}C NMR Characterization. As described previously,[6−8] 100 MHz ^{13}C NMR spectra were obtained on a Varian Unity 400 MHz spectrometer in a 10 mm probe on 10−20 wt % solutions of the polymers and 0.05 M CrAcAc in 1,2,4-trichlorobenzene (TCB) unlocked at 120−140 °C using a 90° pulse of 17.8 μs, a spectral width of 35 kHz, a relaxation delay of 5 s, an acquisition time of 0.64 s, and inverse gated decoupling. Samples were preheated for at least 15 min before acquiring data. Data acquisition time was typically 6−10 h per sample. The T_1 values of the carbons of a polyethylene sample were measured under these conditions to be all less than 0.9 s. Spectra are referenced to the solvent TCB high field resonance at 127.9 ppm. The 2D INADEQUATE data were obtained on a Varian Unity Plus 500 MHz NMR spectrometer at 60 °C using a 10 mm probe, a relaxation delay of 0.76 μs, a 90° pulse of 15.9 μs, a spectral width of 4.3 kHz, an acquisition time of 0.24 s, 800 transients per increment, 158 increments, and folding in f_1 for a total time of about 4 days on a sample consisting of 2.33 g of polymer and 60 mg of CrAcAc with benzene-d_6 in a total volume of 3.1 mL.

Light Scattering (SEC/LS). Intensity light scattering measurements were obtained on all seven polymers using a multiangle light scattering instrument (Wyatt Technology). Measurements were made on highly dilute fractions eluting from a size exclusion chromatograph consisting of a Waters Alliance 2690 solvent delivery system/autoinjector with an in-line solvent degasser, temperature-controlled column compartment, and a Waters 410 differential refractometer. Two 30 cm columns were used (Polymer Laboratories Mixed C, 5 μm particle size). The mobile phase was tetrahydrofuran (THF) stabilized with 0.025% BHT; the flow rate was 0.5 mL/min. The columns were held at 40 °C and the differential refractometer at 35 °C. The mass of the polymer injected onto the column varied with the molecular weight and size of the polymer; typically 50−200 μL of a 5−10 mg/mL solution was injected. Software from Wyatt Technology was used to acquire data from the 18 scattering angles (detectors) and the differential refractometer.

To facilitate comparison of these unique polyethylenes with more familiar semicrystalline polyethylenes, SEC/LS measurements were also performed at 150 °C in trichlorobenzene (TCB). For these measurements, a Polymer Laboratories 210 high-temperature size exclusion chromatograph was used. This instrument also is equipped with a differential refractive index detector, an on-line degasser, and an autoinjector. A Viscotek 210 differential viscometer was also installed within the heated column compartment. Columns used were 4 30 cm Polymer Laboratories Mixed B (10 μm particle size). A high-temperature Dawn DSP (Wyatt Technology) equipped with an Ar ion laser was used for on-line light scattering. The eluent from the columns was directed outside of the PL 210 to the Dawn through a heated transfer line controlled by the Dawn and then back into the 210 into a splitting device permitting parallel detection by the differential refractometer and viscometer. Oxidative degradation was minimized by addition of 0.05% BHT to all TCB used.

The molecular weight M and the root-mean-square radius of gyration, R_g, are evaluated at selected intervals along the distribution eluting from the column using the well-known expressions of classical light scattering:

$$\frac{Kc}{R(\Theta)} = \frac{1}{MP(\Theta)} + 2A_2c + ... \quad (1)$$

where

$$P^{-1}(\Theta) = 1 + \frac{16\pi^2 n^2 R_g^{\ 2} \sin^2(\Theta/2)}{3\lambda^2} + ... \quad (2)$$

and

$$K = \frac{4\pi^2 n^2 (dn/dc)^2}{\lambda^4 N_A} \quad (3)$$

The symbols above have their usual meanings: λ is the wavelength of the incident light, 632.8 nm (or 488 nm for the Ar ion laser), n is the refractive index of the solvent, 1.404 for THF, 1.57 for TCB at 150 °C, and $R(\Theta)$ is the excess Rayleigh factor (minus the solvent) at scattering angle Θ. The concentration c of the polymer at each point on the chromatogram and the differential refractive index increment dn/dc may be determined in one of three ways: (1) equating the integrated refractive index peak to the known mass of the polymer injected and using a known dn/dc, (2) using the calibration of the differential refractometer and a known dn/dc to calculate the mass from the integrated area, and (3) using the calibration of the differential refractometer and the known mass to calculate dn/dc from the integrated area. By using method 3, $dn/dc = 0.078 \pm 0.003$ is obtained for these polymers in THF. The wavelength of the incident light in the differential refractometer is 932 nm; the Dawn DSP uses a HeNe laser at 632.8 nm. No correction for the wavelength dependence, which is expected to be small, was used. For example, Fetters et al.[13] report 0.0696 mL/g at 436 nm and 0.0672 mL/g at 633 nm for poly(ethylethylene) in cyclohexane, a difference of only 3%. The dn/dc of 0.078 is in good agreement with the value of 0.0789 reported by Fetters et al.[14] for atactic polypropylene in THF and with the value of 0.0788 reported by Mays, Hadjichristidis, and Fetters for poly(2-methyl-1-butenylene) in THF[15] in their extensive studies on soluble, model short-chain branched polyolefins. Although the poly(2-methyl-1-butenylene) (an alternating copolymer of ethylene and propylene) has only $^1/_2$ as many methyl branches as the atactic polypropylene, the reported dn/dc are virtually the same. Somewhat larger values were reported by Fetters et al. in a later publication[16] for atactic polypropylene (0.0844) and poly(ethylethylene) (0.0830). These larger values were obtained in freshly distilled THF. Here we have used HPLC grade THF stabilized with BHT to minimize the variation in refractive index that is typically observed for nonstabilized THF. The dn/dc in TCB at 150 °C was evaluated in the same manner and was determined to be -0.100 ± 0.003. The dn/dc of a polymer in a variety of solvents can be approximated using the Gladstone−Dale relation:[18]

$$\frac{dn}{dc} = v_{sp}(n_{pol} - n_{solv}) \quad (4)$$

where v_{sp} is the partial specific volume of the polymer in the solvent, and n_{pol} and n_{solv} are the refractive indices of the polymer and solvent, respectively. Data for dn/dc of a variety of polyethylenes in various solvents from this study and several literature references are shown in Figure 1. The specific volume obtained from the slope is 1.13 mL/g, indicating that minimal error is introduced in approximating the partial specific volume in a variety of solvents by the reciprocal melt density of 0.885 g/mL. Small differences in dn/dc arising from contributions of the methyls from branches and/or low M polymer, differences in temperature, and in incident wavelength are not expected to introduce errors greater than 10% in M determinations and have been neglected. It should be noted that large differences in film density which reflect the degree of branching via the degree of crystallinity are not applicable to these dilute solutions.

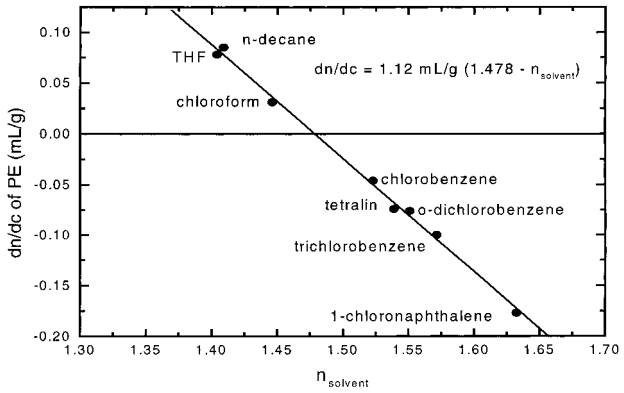

Figure 1. d*n*/d*c* of polyolefins in a variety of solvents.

The weight-average molecular weight, M_w, was obtained from light scattering. For these measurements on fractions eluting from a size exclusion chromatograph, the polydispersity at each "slice" along the chromatogram is expected to be very small; therefore, $M_w \sim M_n$, and the subscripts are omitted. Concentrations of eluting polymer were typically very small (less than 0.3 mg/mL), so that the second term in eq 1 is neglected.

For polymers 2 and 7, determination of the weight-averaged molecular weight, M_w, the root-mean-square radius of gyration, $R_{g,z}$, and the second virial coefficient, A_2, was made with intensity light scattering measurements on the unfractionated polymer at higher concentrations. For these measurements, a Brookhaven Instruments goniometer was used. Five concentrations were prepared in the dilute region, and measurements were made using an Ar ion laser at 488 nm.

Hydrodynamic Measurement. In addition to intensity light scattering, hydrodynamic dimensions of some of these unfractionated polymers were also determined: the Stokes radius from dynamic light scattering and the intrinsic viscosity. Dynamic light scattering was performed using a Brookhaven Instruments goniometer (200SM) and a BI9000AT correlator. The Stokes radius, R_H, was calculated from the limiting diffusion coefficient at infinite dilution and zero scattering angle:

$$D_0 = \frac{kT}{6\pi\eta_0 R_H} \tag{5}$$

where

$$D_0 = \lim_{c\to 0,\theta\to 0} D_M \tag{6}$$

and D_M is evaluated by the method of cumulants (second-order polynomial), using software from Brookhaven Instruments. Measurements were done at 3−4 scattering angles; results were independent of scattering angle within experimental uncertainty.

The intrinsic viscosity, $[\eta]$, was determined using a Viscotek dual-capillary viscometer as a detector with a size exclusion chromatograph. Measurements were done at 40 °C in THF and at 150 °C in TCB with the Polymer Labs 210. The THF results were obtained separately from the SEC/LS results, using a different instrument. For these results, $[\eta]$ and M were obtained using Viscotek software; M was obtained from a universal calibration curve established with polystyrene standards. The viscosity in TCB was obtained simultaneously with the light scattering as described above. The differential viscometer signal was read as an additional auxiliary detector using the Wyatt software.

Results

1. SEC/LS. Figure 2 shows a typical 3-D plot of the light scattering chromatograms at 16 scattering angles, along with the refractive index chromatogram for no. 2. The scattering intensity, proportional to the product

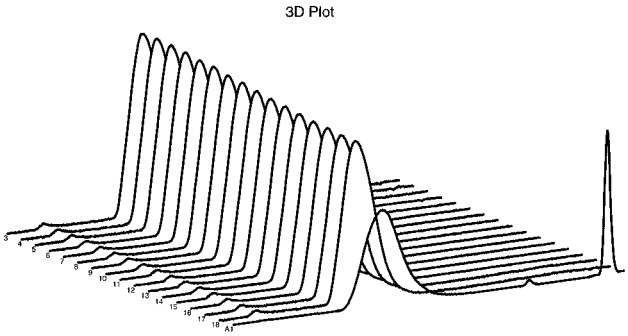

Figure 2. Light scattering (detectors 3−18) and refractive index (A1) chromatograms for polymer 2 in THF.

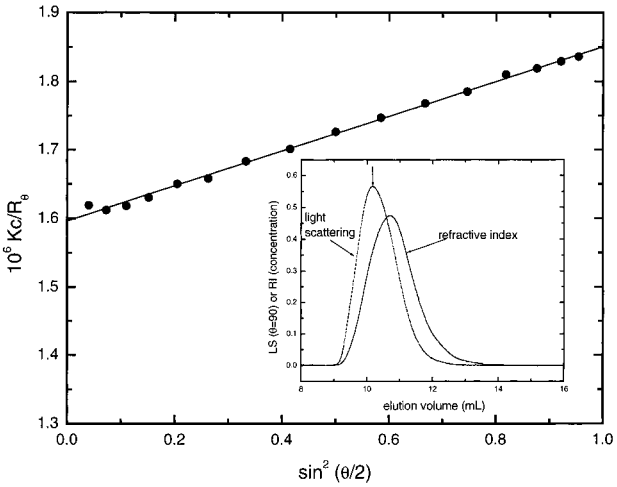

Figure 3. Angular dependence of Kc/R_Θ at a single "slice" of the eluting distribution of polymer 2, as indicated.

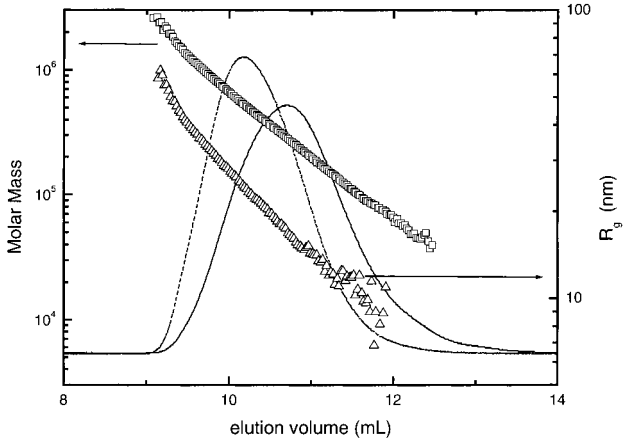

Figure 4. Molar mass and R_g calculated from the light scattering and refractive index chromatograms across the distribution for polymer 2.

of concentration and M, exhibits much greater intensity in the high-M, early eluting portion of the distribution relative to the refractive index chromatogram, which is proportional only to the concentration. The chromatograms at higher scattering angles (larger detector numbers) exhibit reduced intensity due to intramolecular interference. Thus, both M and R_g may be evaluated at chosen points across the distribution, as shown in Figures 3 and 4. Figure 3 shows the angular dependence at one "slice" on the chromatogram as indicated. Values of M and R_g are evaluated at each "slice" using the equations above. Both log M and log R_g exhibit a linear dependence on elution volume as shown in Figure 4. For

Table 1. Dilute Solution Parameters Obtained in THF

polymer	1	2	3	4	5	6	7
E pressure	0.1 atm	1 atm	25 psi	50 psi	100 psi	250 psi	500 psi
$M_{w,SEC-LS}$	155000	480000	300000	270000	440000	370000	440000
M_z/M_w	1.49	1.58	1.35	1.38	1.34	1.32	1.38
$R_{g,w,SEC-LS}$ (nm)		21.0	19.7	18	27.1	25.2	31.9
$R_{g,z,SEC-LS}$ (nm)	~7	25.8	22.8	23	32.0	30.7	37.5
$10^4(R_{g,w}^2/M_w)_{SEC-LS}$	3	9	12.8	12	16.7	17.2	23
$R_{g,z,LS}$ (nm)		26.0					36.3
R_{A2} (nm)		23					30
10^4A_2 (mL mol/g^2)		1.3					3.6
$M_{w,LS}$		480000					450000
R_H (nm)	8	16.7	11.8				18.7
$R_{g,w}/R_H$	~0.9	1.3	1.6				1.7
k_D (mL/g)	−10	−9	14				34
$[\eta]_{SEC-\eta}$ (mL/g)	16.9	60.6					171.4
$R_{g,\eta}$ (nm)	8	16.3					23
α	0.3	0.6					0.56

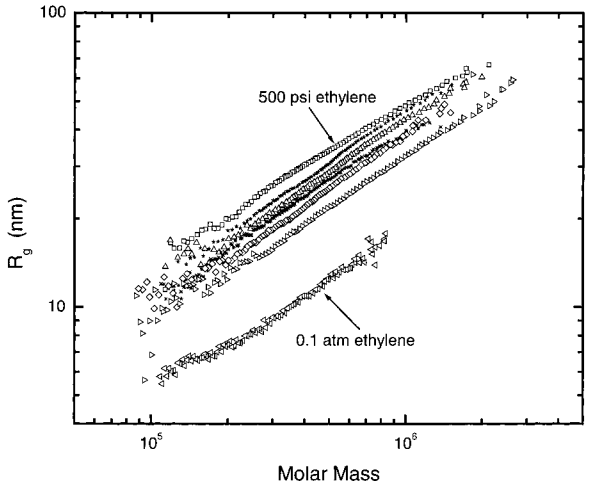

Figure 5. R_g as a function of M across the distribution for all seven polymers synthesized at varying ethylene pressure, in THF at 40 °C.

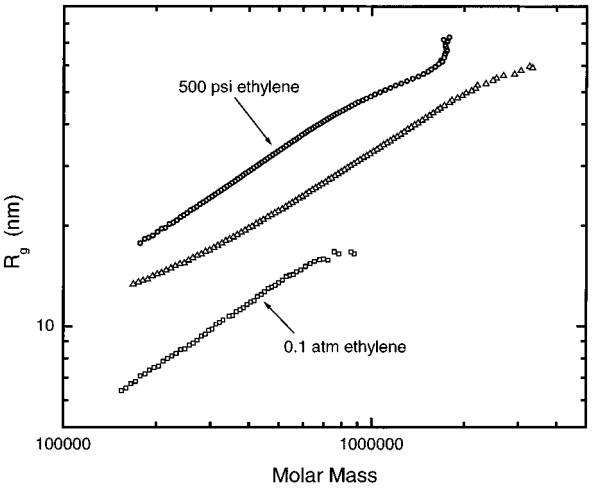

Figure 6. R_g as a function of M for polymers 1, 2, and 7 in TCB at 150 °C.

typical polydispersities, this provides M and R_g of narrow fractions over more than a decade in M, as shown in Figure 5 for THF and Figure 6 for TCB at 150 °C. The linear dependencies of log M and log R_g are indicative of separation by size exclusion, with no evidence of competing separation mechanisms or column overloading. These effects can frequently be detected as nonlinear dependencies on elution volume in these plots.

The data obtained for the polyethylene synthesized at the lowest ethylene pressure (0.1 atm) require additional comment. Observation of Figures 5 and 6 indicates that this polymer, despite its substantial molecular weight (M_w of about 150 000, see Table 1), has a very small R_g, which is a consequence of the very highly branched topography of this polymer. Experimental determination of R_g less than about 10 nm using light scattering usually cannot be accomplished with reasonable accuracy. This is because the disymmetry over the entire angular range for a R_g less than about 10 nm will be only about 2% of the scattered intensity. Typically, scattered intensities may only be determined within about 1%. Light scattering on dilute polymer solutions eluting from a chromatographic column offers some experimental advantages that substantially reduce the problems of extraneous scattering: (1) the detectors at the various scattering angles are fixed, (2) the continuous flow of solvent and/or solution greatly minimizes the dust present at the air/liquid interface, (3) the chromatographic column acts as a highly efficient "filter" to remove particulates, and (4) the scattering volume is very small. In addition, the highly branched polymer is quite high in segment density. This polymer could be analyzed at much higher concentration than typical linear polymers of similar M, which also facilitated determination of R_g. With these advantages, R_g for the portion of the distribution with $M > 100\,000$ could be estimated, as shown in Figures 5 and 6. In Figures 5 and 6, the lower half of the distribution has been omitted for the 0.1 atm polymer, since R_g could not be estimated at these lower M. Data obtained in TCB at higher temperature could be extended to somewhat lower M for several reasons: (1) incident light was 488 nm instead of 633 nm, (2) dn/dc is larger in magnitude in TCB, and (3) the four Mixed B columns permitted a larger concentration to be used. The estimate of R_g from light scattering with size exclusion chromatography is in reasonable agreement with the determination from neutron scattering in toluene-d_8.[19]

The weight-average molecular weight, M_w, a higher order polydispersity index, M_z/M_w, and the weight and z-averages of the root-mean-square radius of gyration, $R_{g,w}$, and $R_{g,z}$, are listed for all seven polymers in Table 1. Table 3 lists the same parameters for polymers 1, 2, and 7 in TCB at 150 °C. The ratio M_z/M_w was chosen as an indication of the polydispersity rather than the more familiar M_w/M_n since M_n reflects the lowest molecular weight portion of the distribution, where light scattering results are most uncertain. For all seven polymers, $M_w/M_n = 1.7 \pm 0.2$. These parameters are averaged over the entire distribution by summation over

Table 2. Short Chain Branching Distribution from ^{13}C NMR, Number of Branches per 1000 CH_2

polymer	1	2	3	4	5	6	7
E pressure	0.1 atm	1 atm	25 psi	50 psi	100 psi	250 psi	500 psi
total Me	122	123	118	122	118	117	114
Me	38.9	39.3	38.7	40.9	40.2	42.3	41.5
Et	28.8	29.6	28.1	28.7	26.8	25.8	23.1
Pr	3.0	3.1	2.7	2.9	3.0	3.6	4.4
Bu	12.1	12.1	11.9	11.9	11.9	11.4	9.3
Am	3.6	2.3	2.8	3.2	3.2	3.8	4.6
hexyl and higher (including EOC)	36.3	36.3	34.6	34.8	34.2	31.9	31.9
% 1B, methyls in *sec*-butyl branches	24.2	21.2	20.1	19.6	17.3	15.8	14.8

Table 3. Dilute Solution Parameters Obtained in TCB at 150 °C

polymer	1	2	7
E pressure	0.1 atm	1 atm	500 psi
$M_{w,SEC-LS}$	156000	500000	465000
M_z/M_w	1.38	1.51	1.37
$R_{g,w,SEC-LS}$ (nm)		23.0	32.1
$R_{g,z,SEC-LS}$ (nm)	~9	28.6	38.2
$10^4(R_{g,w}^2/M_w)_{SEC-LS}$	5	10.6	22
$[\eta]_{SEC-\eta}$ (mL/g)	17.6	66	185
$R_{g,\eta}$ (nm)	8	17	24
α	0.43	0.70	0.74

the "slices". It should be noted that elution volume exhibits a logarithmic dependence on molecular weight, so that "slices" of equal volume encompass progressively broader regions at higher molecular weight.[20] Figures 5 and 6 show that for all seven polymers $R_g \propto M^{0.5}$, within experimental uncertainty. This permits use of $R_{g,w}^2/M_w$ as a molecular weight independent parameter characteristic of the structure. These measurements are obtained in thermodynamically favorable solvents for the polyethylenes, and no corrections have been done for excluded-volume interactions. These interactions are expected to expand the polymer dimensions from the unperturbed state. However, these polymers are all highly branched, and the long-range interactions are reduced; the decrease in $R_{g,w}^2/M_w$ as a function of ethylene pressure primarily reflects the changing topography of the branching. This parameter is also listed in Tables 1 and 3 and is seen to vary by nearly an order of magnitude for the range of ethylene pressures employed.

2. Light Scattering. Intensity light scattering measurements were also made on two of the unfractionated polymers over a larger concentration range as described above. Results in the form of a Zimm plot for polymer 2 are shown in Figure 7. The weight-average molecular weight, M_w, and *z*-average root-mean-square radius of gyration, R_g, were in good agreement with the corresponding averages obtained by summation of the "slices" in the SEC/LS measurements, as shown in Table 1. The second virial coefficient, A_2, listed in Table 1 decreases for polymers synthesized with reduced ethylene pressure.

3. SEC/η. The intrinsic viscosities listed in Tables 1 and 3 were obtained by integration of the relative viscosity and refractive index (concentration) chromatograms obtained from SEC with viscosity detectors. The dependence of $[\eta]$ on M across the distribution for three of the polymers is shown in Figure 8 for both THF and TCB at 150 °C. In contrast to the R_g dependence on M shown in Figures 5 and 6, where the slopes are parallel for all the polymers, the dependence of $[\eta]$ on M shown in Figure 8 exhibits a reduced slope for the most compact polyethylene obtained at very low ethylene pressure. The exponent, α, in the Mark−Houwink

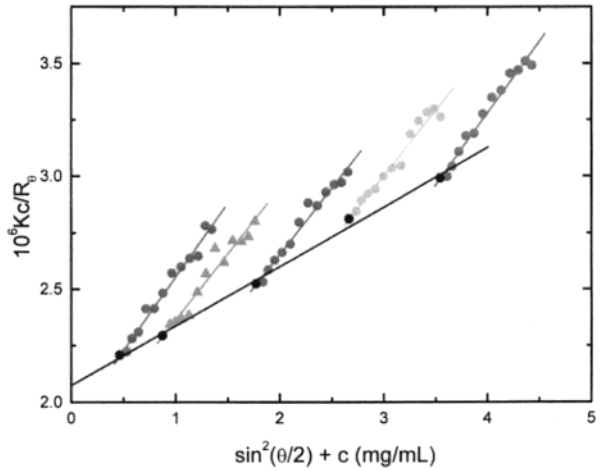

Figure 7. Concentration and angular dependence of off-line intensity light scattering for polymer 2 in THF.

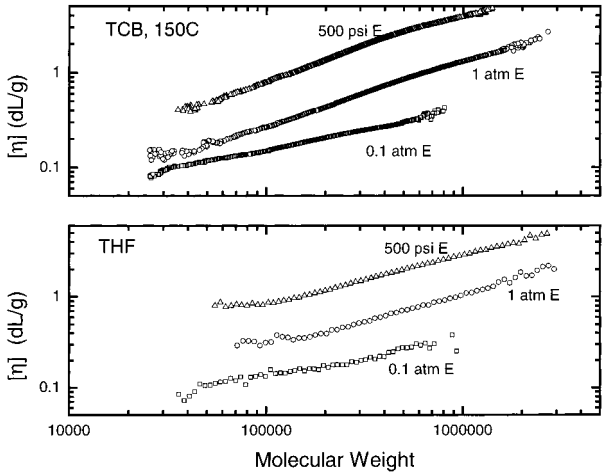

Figure 8. Intrinsic viscosity $[\eta]$ as a function of M for polymers 1, 2, and 7 in THF at 40 °C and in TCB at 150 °C.

relation is also listed in Tables 1 and 3. In Figure 8, the molecular weights in THF are obtained from the elution volume using a universal calibration approach. The molecular weights in TCB were obtained directly from the light scattering. Despite this significant difference in experimental technique, the results are very consistent, and the reduced exponent α for the most densely branched polymer is observed in both sets of data. This is discussed further below.

4. Dynamic Light Scattering. The hydrodynamic radius, R_h, for four of the polymers in THF is listed in Table 1. The dependence of the mutual diffusion coefficient, D_M, on concentration reflects both thermodynamic effects and frictional effects:

$$D_M(c) = \frac{kT}{f(c)}(1 - \nu c)\frac{\partial \pi}{\partial c} \qquad (7)$$

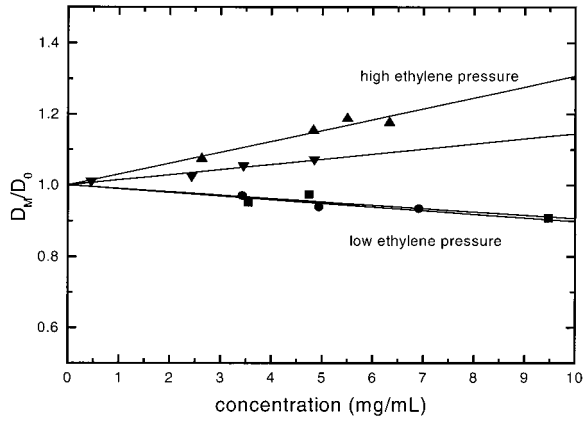

Figure 9. Reduced diffusion coefficient D_M/D_0 as a function of concentration for polymers 1, 2, 3, and 7.

with the thermodynamic dependence contained in the osmotic compressibility, $\partial\pi/\partial c$, and the hydrodynamic dependence in the concentration dependence of the friction coefficient, $f(c)$

$$f(c) = f_0(1 + k_f c + ...)$$

where k_f is usually positive. Combining these, and neglecting higher order terms, a simplified expression can be used at high dilutions:

$$D_M = D_0(1 + k_D c) \tag{8}$$

where

$$k_D = 2A_2M - k_f - \nu$$

The second virial coefficient, A_2, and the frictional dependence vary with polymer structure. Thus, for typical linear, flexible polymers, k_D is positive in thermodynamically good solvents where the positive A_2 term dominates and becomes negative in marginal or poor solvents, when A_2 is small. Similarly, A_2 is also small for highly branched polymers, where long-ranged interactions are minimized. Figure 9 exhibits the change in sign of k_D for these polymers as a function of ethylene pressure during synthesis. At higher ethylene pressures where a predominantly linear topography is obtained, k_D is positive. As ethylene pressure is reduced, the topography becomes much more densely branched, A_2 becomes very small, and k_D is dominated by the frictional dependence and is negative.

5. ^{13}C NMR. The highly branched polyethylenes synthesized with these and similar catalysts exhibit a rich spectrum of branching structures.[6−11,21] Figure 10 shows the spectrum obtained for sample 5, synthesized at 100 psi ethylene. Unique carbon resonances can be identified for the methyl through amyl short chain branches and also for the class of branches hexyl and longer.[6−8] These allow us to determine the amount of each of these branches per 1000 CH_2 in the polymers, as listed in Table 2. For this measurement, we define a branch length as the number of carbons from and including a methyl to the nearest methine, including the intervening methylenes; thus, one *sec*-butyl branch would contribute one methyl and one ethyl branch to the listed total of ethyl and methyl branches. The total methyl groups per 1000 C is very high (around 120, see Table 2). In addition to the known methyl resonances for the various short chain branches, we observe two

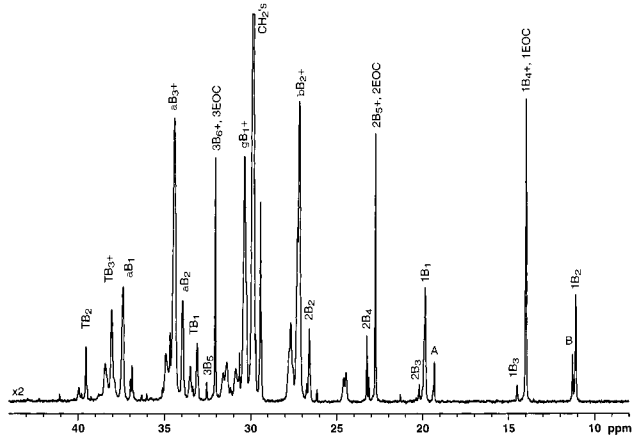

Figure 10. ^{13}C 400 MHz NMR spectrum of polymer 5 (100 psi E) at 120 °C. Polymer is 15 wt % in 1,2,4-trichlorobenzene with 0.05 M CrAcAc, referenced to TCB high-field resonance at 127.9 ppm. Note on labels xB$_y$ B$_y$ is a branch of length y carbons; x is the carbon being discussed, and the methyl at the end of the branch is numbered 1. Thus, the second carbon from the end of a butyl branch is 2B$_4$. xB$_y$+ refers to branches of length y and longer. When x in xB$_y$ is replaced by a T, the methine carbon of that branch is denoted. The methylenes in the backbone are labeled with Greek letters which determine how far from a branch point methine each methylene is; α denotes the first methylene next to the methine. Thus, γB$_1$+ refers to methylenes γ from a branch of length 1 or longer. EOC is end of chain; 2EOC is the second carbon from the end of the chain (the first methylene). A and B are the methyls of the methyl and ethyl branches, respectively, which comprise the *sec*-butyl ended branch.

methyl resonances not previously observed in any polyethylene, denoted by "A" and "B" in Figure 10. Using 2D INADEQUATE, we have determined that these arise from the two methyls on a *sec*-butyl branch.[6−8] This is the smallest possible "branch-on-branch" structure and is direct evidence that the chain walking mechanism can occur even through a tertiary carbon. The percentage of methyl branches that are on *sec*-butyl branches is listed in Table 2 for each of the seven polymers.

Discussion

^{13}C NMR results for the total methyl end groups per 1000 CH_2 listed in Table 2 indicate very little change in total branching and the distribution of short chain branches over the range of ethylene pressures studied.[6−8] In contrast, the light scattering results indicate that lower ethylene pressures result in a far more compact, highly branched structure. In addition, the polymers synthesized at very low ethylene pressures are typically viscous oils, while those synthesized at high ethylene pressures are tough elastomers. These observations are consistent with the existence of a substantial amount of branch-on-branch structures, which are favored at reduced ethylene pressure. The existence of the smallest branch-on-branch structure, the *sec*-butyl, was previously identified from ^{13}C NMR.[6] This is in agreement with the observation that "chain walking", which gives rise to the branches in the absence of comonomers, can also occur across a tertiary carbon to produce a branch-on-branch. A mechanism in which this process is competing favorably with addition of ethylene at low ethylene pressures provides an explanation for the preponderance of branch-on-branch structures at low ethylene pressures.[6−9] In addition, it explains the relative abundance of short branches with even numbers of carbons when compared to those with odd numbers

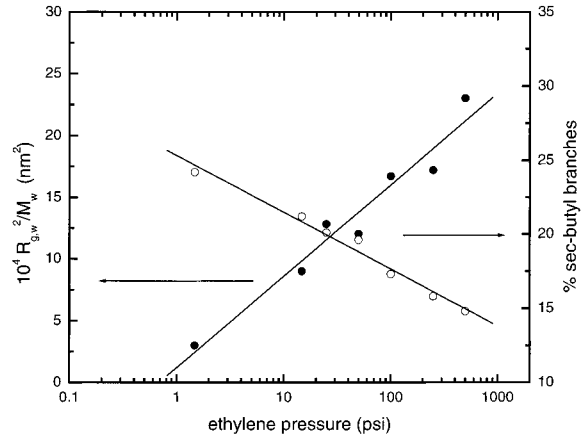

Figure 11. Parameter $R_{g,w}^2/M_w$ and the fraction of methyl branches in *sec*-butyl branches as a function of ethylene pressure during synthesis.

of carbons; that is, the amount of propyl branches is much lower than expected from interpolation between the amounts of ethyl and butyl.[11] Figure 11 displays the dependence of the parameter $R_{g,w}^2/M_w$ and the fraction of methyl branches in *sec*-butyl branches as a function of ethylene pressure during synthesis. Clearly, as the proportion of branch-on-branch species increases, the segment density increases, leading to a the densely branched structure at the lowest ethylene pressure.

Additional direct evidence of the densely branched structure of the polymer formed at very low ethylene pressure is given by the dilute solution properties. The ratio R_g/R_H, also listed in Table 1, reflects the polymer shape independent of M.[20,22] For polydisperse, linear, flexible polymer coils in good solvents, this ratio can be as large as 2. Increasing the segment density, as for rings or branched chains, reduces the ratio. For a "hard sphere", this ratio falls below unity to 0.78.[20,22] Values below unity have been reported for other polymers that are expected to have a high segment density such as multiarm stars,[23] dendrimers,[24] and microgels.[25] Burchard and Kajiwara have calculated the static form factor $P(q)$ and the first cumulant of the time correlation function from dynamic light scattering for the *soft sphere*.[26] This model consists of a centrosymmetric unit of three branches, each of which terminates in another trifunctional branch point (first shell) and so on to successive shells. The polymer chains between shells have a length m; in the limit of $m = 1$, the model reduces to a dendrimer. This model is a closer approximation to the expected structure of the densely branched polyethylene obtained at 0.1 atm ethylene than other possible models such as a star, dendrimer, or hard sphere. The soft sphere model encompasses the limiting cases of a three-arm star for one branching shell and approaches the globular or "hard sphere" case for many branching shells (18 or more for a degree of polymerization of 1 million). In the case of only a few branching shells, as expected for these polyethylenes, R_g^2 increases linearly with M, as observed in Figures 5 and 6. For the soft sphere, Burchard and Kajiwara calculate a ratio R_g/R_H of 0.98 for more than 10 branching shells. The experimental value of R_g/R_H is about 0.9 for the most densely branched polymer (no. 1). The values listed in Table 1 are consistent with a predominantly linear random coil at high ethylene pressures (minimal branch-on-branch) and with the "soft sphere" model at very low ethylene pressure (maximum branch-on-branch).

The "scaling" exponents observed for R_g and $[\eta]$ as a function of M in Figures 5, 6, and 8 merit some comment. The significance of scaling laws in understanding polymer properties provides a temptation to overinterpret an exponent that in many cases is very uncertain and determined over a limited range. It should be noted that these fractions are obtained by size exclusion chromatography and thus may reflect separation mechanisms in addition to changing molecular weight. For example, a distribution of branching topology is expected for these polymers. Assuming separation occurs according to the commonly accepted "hydrodynamic volume", polymers with higher molecular weight but more branch-on-branch (smaller hydrodynamic volume) will coelute with lower M and less branch-on-branch. Several other studies have suggested that branching would influence separation on the basis of entropic considerations.[27,28] Experimental considerations (primarily the interdetector volume) can also influence these exponents. Considering these cautions, we can still observe that the exponents vary little in the R_g dependence of Figures 5 and 6. Similarly, little change in exponent for R_g as a function of M was observed for a series of stars as the number of rays was increased from 2 (linear) to 128.[29] However, the exponent for the most highly branched polymer is substantially reduced in the $[\eta]$ dependence of Figure 8, for both solvents. The intrinsic viscosity is often expressed using the Fox−Flory expression:[30]

$$[\eta] = \Phi\left[\frac{R_g^3}{M}\right]$$

where Φ is a constant for linear, flexible chains. However, Φ reflects the hydrodynamic interaction through the segmental density and is expected to increase with branching. Experimental determination of Φ using the average values of M_w, $R_{g,w}$, and $[\eta]$ listed in Tables 1 and 3 shows an increase in Φ as the branching becomes more dense. For the polymer synthesized at 0.1 atm ethylene, where the topography is very densely branched, the segment density decreases as molecular weight increases, so that Φ decreases with M. A more dramatic example of this has been reported for a series of dendrimers.[31]

A variety of dilute solution measurements have been presented to support the proposed topographical changes in branching structure observed for these highly branched polyethylenes. Recent mechanistic studies by Brookhart and co-workers indicate differences in the energy barriers to migratory insertion for the nickel and palladium catalysts which may be related to the unique topographical variation observed for the palladium-catalyzed polyethylenes.[32] This class of catalysts provides the opportunity for unprecedented control of the branching microstructure and resulting physical properties.

Acknowledgment. We very much appreciate the technical assistance of Joseph Galperin, Jiazhong Chen, Carole Urbston, Peggy Foster, and Mike Enderle in performing the synthesis and measurements reported here. We also appreciate discussions with Sam Arthur, Linda Johnson, Professor Maurice Brookhart (UNC), Mark Teasley, Steve Ittel, and Ralph Fuller.

References and Notes

(1) See for example: Billmeyer, F. W. *Textbook of Polymer Science*; John Wiley and Sons: New York, 1984; p 363.

(2) Ferry, J. D. *Viscoelastic Properties of Polymers;* John Wiley and Sons: New York, 1986. Doi, M.; Edwards, S. F. *The Theory of Polymer Dynamics;* Oxford University Press: Oxford, 1986.
(3) Kaminsky, W.; Arndt, M. *Adv. Polym. Sci.* **1997**, *127*, 143.
(4) Johnson, L. K.; Killian, C. M.; Brookhart, M. *J. Am. Chem. Soc.* **1995**, *117*, 7, 6414.
(5) Mohring, V.; Fink, G. *Angew. Chem.* **1985**, *97*, 982.
(6) McLain, S. J.; McCord, E. F.; Johnson, L. K.; Ittel, S. D.; Nelson, L. T. J.; Arthur, S. D.; Halfhill, M. J.; Teasley, M. F.; Tempel, D. J.; Killian, C.; Brookhart, M. S. *Polym. Prepr.* **1997**, *38* (1), 772.
(7) Guan, Z.; Cotts, P. M.; McCord. *Polym. Prepr. (Am. Chem. Soc.)* **1998**, *39* (2), 402.
(8) Guan, Z.; Cotts, P. M.; McCord, E. F.; McLain, S. J. *Science* **1999**, *283*, 2059.
(9) Jurkiewicz, A.; Eilerts, N. W.; Hsieh, E. T. *Macromolecules* **1999**, *32*, 5471.
(10) Ittel, S. D.; Johnson, L. K.; Brookhart, M. *Chem Rev.* **2000**, *100*, 1169−1203.
(11) Gates, D. P.; Svejda, S. A.; Onate, E.; Killian, K. M.; Johnson, L. K.; White, P. S.; Brookhart, M. S. *Macromolecules* **2000**, *33*, 2320.
(12) Mader, D.; Heinemann, J.; Walter, P.; Mulhaupt, R. *Macromolecules* **2000**, *33*, 1254.
(13) Zhongde, X.; Hadjichristidis, N.; Carella, J. M.; Fetters, L. J. *Macromolecules* **1983**, *16*, 925.
(14) Zhongde, X.; Mays, J.; Xuexin, C.; Hadjichristidis, N.; Schilling, F. C.; Bair, H. E.; Pearson, D. S.; Fetters, L. J. *Macromolecules* **1985**, *18*, 2560.
(15) Mays, J.; Hadjichristidis, N.; Fetters, L. J. *Macromolecules* **1984**, *17*, 7, 2723.
(16) Zirkel, A.; Urban, V.; Richter, D.; Fetters, L. J.; Huang, J. S.; Kampmann, R.; Hadjichristidis, N. *Macromolecules* **1992**, *25*, 6148.
(17) Kim, J. S.; Pawlow, J. H.; Wojcinski, L. M. II; Murtuza, S.; Kacker, S.; Sen, A. *J. Am. Chem. Soc.* **1998**, *120*, 1932. Murtuza, S.; Harkins, S. B.; Long, G.; Sen, A. *J. Am. Chem. Soc.* **2000**, *122*, 1867.
(18) See for example: Huglin, M. B. In *Light Scattering from Polymer Solutions;* Huglin, M. B., Ed.; Academic Press: London, 1972; Chapter 6.
(19) Cotts, P. M.; Guan, Z.; Co, C.; Kaler, E., unpublished results.
(20) Burchard, W. *Adv. Polym. Sci.* **1999**, *143*, 113.
(21) Galland, G. B.; de Souza, R. F.; Mauler, R. S.; Nunes, F. F. *Macromolecules* **1999**, *32*, 1620.
(22) Buchard, W. *Adv. Polym. Sci.* **1983**, *48*, 1.
(23) Bauer, B. J.; Fetters, L. J.; Graessley, W. W.; Hadjichristidis, N.; Quack, G. F. *Macromolecules* **1989**, *22*, 2337.
(24) Scherrenberg, R.; Coussens, E.; van Vliet, P.; Edouard, G.; Brackman, J.; de Brabander, E.; Mortensen, K. *Macromolecules* **1998**, *31*, 456.
(25) Kunz, D.; Thurn, W.; Burchard, W. *Polym. Colloid Sci.* **1983**, *261*, 635.
(26) Burchard, W.; Kajiwara, K.; Nerger, D. *J. Polym. Sci., Polym. Phys. Ed.* **1982**, *20*, 157.
(27) Casassa, E. F. *J. Polym. Sci., Polym. Lett. Ed.* **1967**, *5*, 773.
(28) Casassa, E. F.; Tagami, Y. *Macromolecules* **1969**, *2*, 14.
(29) Roovers, Z.; Zhou, L.-L.; Toporowski, P. M.; van der Zwan, M.; Iatrou, H.; Hadjichristidis, N. *Macromolecules* **1993**, *26*, 4324.
(30) Flory, P. J.; Fox, T. G. *J. Am. Chem. Soc.* **1951**, *73*, 1904.
(31) Mourey, T. H.; Turner, S. R.; Rubinstein, M.; Frechet, J. M. J.; Hawker, C. J.; Wooley, K. L. *Macromolecules* **1992**, *25*, 2401.
(32) Huff, R. L.; Svejda, S. A.; Tempel, D. J.; Leatherman, M. D.; Johnson, L. K.; Brookhart, M. *Polym. Prepr.* **2000**, *41* (1), 410.

MA000926R